THE JOURNAL OF PHYSICAL CHEMISTRY B
A JOURNAL OF THE AMERICAN CHEMICAL SOCIETY

pubs.acs.org/JPCB

Article

Phase-State-Dependent Silica Nanoparticle Uptake of Giant Unilamellar Vesicles

Manuel M. Sirch, Andrej Kamenac, Simon V. Neidinger, Achim Wixforth, and Christoph Westerhausen*

Cite This: J. Phys. Chem. B 2024, 128, 7172−7179

Read Online

ACCESS | Metrics & More | Article Recommendations

ABSTRACT: We quantify endocytosis-like nanoparticle (NP) uptake of model membranes as a function of temperature and, therefore, phase state. As model membranes, we use giant unilamellar vesicles (GUV) consisting of 1,2-dipentadecanoyl-sn-glycero-3-phosphocholine (15:0 PC). Time-series micrographs of the vesicle shrinkage show uptake rates that are a highly nonlinear function of temperature. A global maximum appears close to the main structural phase transition at $T = T_m + 3$ K = 37 °C and a minor peak at the pretransition $T = T_p = 22$ °C. The quality of linear fits to the shrinkage, and thus uptake kinetics, reveals a deviation from the linear trend at the vesicle shrinkage peaks. Taking values for the bending modulus as a function of temperature from literature and Helfrich's model allows us to draw qualitative conclusions on the membrane tension and the adhesion of the NP to the membrane as a function of temperature. These findings provide valuable insights into the dynamic interplay between temperature, membrane phase transitions, and NP uptake, shedding light on the complex behavior of biological membranes.

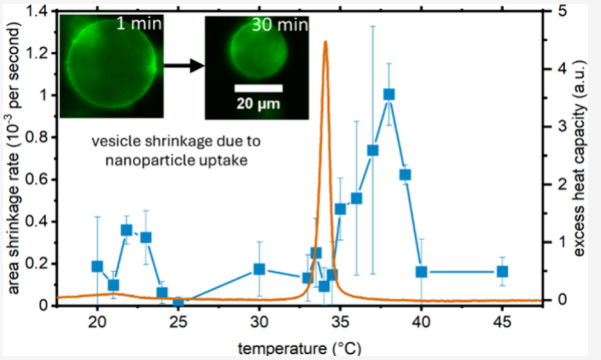

INTRODUCTION

Cell exposure to nanoparticles (NP) has been studied for medical benefits, such as coatings for implants,[1−3] drug delivery carriers,[4−7] tumor imaging,[8] antibacterial agents,[9] and nanomedicine.[10−12] However, potential harms have also been documented, as NP are found in cosmetics, paints, and printer toners.[13−15] Reported undesirable effects include toxicity, coagulatory effects,[16] and pregnancy complications.[17] These studies fall into three categories: in vivo studies providing a macroscopic view, such as LD50 values[18] and biodistribution[19]; in vitro studies showing no NP uptake at 4 °C compared to 37 °C,[20,21] with toxicity linked to material chemistry[22]; and fundamental research on membrane models and artificial membranes to understand NP-cell interactions.[23−27]

This paper addresses phase-state-dependent silica NP uptake of giant unilamellar vesicles (GUV), filling the gap in systematic studies on NP uptake as a function of phase state. By investigating temperature variations using 60 nm silica NP and 15:0PC GUV, we aim to elucidate the underlying mechanisms. To understand these mechanisms, the theory needs to be explained as follows.

Helfrich published a physical model of NP engulfment based on three major energetic contributions: adhesion energy (E_{adh}) as the driving force, bending energy (κ) and tension energy (σ) as the opposing forces.[28,29] Based on the interplay of these mechanical contributions, three different regimes of nanoparticle−membrane interaction were identified: repulsion, partial engulfment, and full engulfment. More recent and sophisticated experimental and theoretical work has been done by Lipowsky.[23,30] Repulsion appears when the adhesion energy is below a threshold given by the bending modulus of the membrane and the particle radius. For partial engulfment, the adhesion energy exceeds this lower limit but does not reach an upper limit $r_{c,\sigma} = \frac{2\kappa}{E_{adh} - \sigma}$, above which full engulfment appears. When fully engulfed, the NP separates from the membrane by fission of the membrane neck and creates a membrane defect, a transient pore, which heals after its characteristic lifetime. Typical lifetimes vary in the range of $t \approx 100$ ms,[31] but can be significantly increased by the addition of substances, like another type of lipid or polymers.[32] Pore lifetimes in cells are longer than in artificial membranes, as commonly reported in the seconds to minutes regime.[33,34,35] The amount of work to form a pore is proportional to the isothermal compressibility, which is minimal at the structural phase transition. Thus, in this regime, pore formation is facilitated.[36] Pores give opportunity to fluid flow, which reduces membrane tension

Received: April 11, 2024
Revised: June 18, 2024
Accepted: July 3, 2024
Published: July 12, 2024

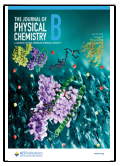

https://doi.org/10.1021/acs.jpcb.4c02383
J. Phys. Chem. B 2024, 128, 7172−7179

in vesicles. The relation $\lambda = \frac{2\kappa}{\sigma}$ gives a good estimate whether the bending ($\lambda > 1$) or the tension ($\lambda < 1$) is the dominating opposing mechanism.[37]

The first key parameter, the bending modulus, for a fluid membrane, e.g., DOPC at room temperature, can be estimated to $\kappa = 10^{-19}$ J.[38] However, close to a structural phase transition, the bending modulus, just as all other susceptibilities is not constant, instead, it is highly nonlinear.[39−42] Heimburg calculated the bending modulus and found a dip in the bending modulus as a function of temperature in the melting transition.[39] Some experimental studies using DMPC and DPPC GUV measure the bending modulus in the melting regime and above, but not at lower temperatures.[40,41] In contrast to Heimburg, they observe an anomaly within $T_m < T \leq T_m + 6$ K. Within $T \leq T_m + 3$ K, the bending modulus first rises to a prominent maximum, until it decreases until for $T \leq T_m + 6$ K to a temperature-independent limit for both DMPC and DPPC.[40] Interestingly, cholesterol, well-known to suppress first-order lipid phase transitions, increases the bending modulus and diminishes the prominent maximum.[41]

New measurements show the bending modulus in the gel state is an order of magnitude higher than in the fluid state.[43] The bending modulus, κ, remains constant at 10^{-18} J in the gel phase and 10^{-19} J in the fluid phase. However, during structural phase transitions and in the ripple phase, the bending energy is nonlinear. At the main structural phase transition and pretransition, κ dips, while in the ripple phase, it rises linearly from 10^{-19} to 10^{-18} J. These findings are likely applicable to cells, as minor changes in membrane composition do not significantly affect the bending modulus, as seen in the similarity between red blood cell membranes and vesicles.[44]

However, structural phase transitions in artificial lipid bilayers are similar to, but not identical to phase transitions of cells. The existence of phase transitions in organisms, like *Escherichia coli*, lung surfactant, or fibroblast cells has been well-known since the 1970s.[45] A recent study by our group has revealed, that the width of the phase transition in biological membranes is much higher.[46] Consequently, many more cell types might display structural phase transitions than reported in the literature, as commonly only a narrow window around $T = 37$ °C is investigated. Despite the broadness of the transition on the scale of a cell population, the width is expected to be sharper on the single-cell scale, and even sharper for local lipid domains, which has been visualized by Yamamoto and Ando[47] and shown exemplarily by Fedosejevs and Schneider.[48]

The dependence of the bending modulus is controlled by the hydrophobic part of the lipid bilayer.[49] The quantitative behavior of the bending modulus has been found to follow a power law of the packing parameters.[50] As the melting transition consists of structural changes, such as a change in area and volume per lipid molecule,[51] a change in the bending modulus is expected.

A great simplification and model view for bending is the compression and expansion of the outer and inner monolayers, respectively. Expansion and compression result in a change in lateral pressure π, which the Clausius−Clapeyron relation $\frac{dT_m}{d\pi} = T_m \frac{\Delta A}{\Delta H}$ directly links to a change in the melting temperature, where ΔH is the enthalpy and ΔA is the change in area.[52] Consequently, all susceptibilities change in phase, as all thermodynamic susceptibilities are coupled.[53,54]

The second key parameter, membrane tension, is characterized by two regimes. In the low-tension regime, the tension rises exponentially with increasing area dilation, and at the same time, thermal fluctuations become restricted. In the high-tension regime, the dependence is linear, as the area-per-molecule expands directly.[55] Membrane tension has been experimentally proven to exist for example in red blood cells[44] and changes drastically, e.g., in diameter changing blood vessels, like capillaries, or during the adhesion process of any type of molecule or NP.

The third key parameter, adhesion, strongly depends on the material of the NP.[56] Silica is one of the most commonly used materials for NP in applications such as drug delivery vehicles and others. Several reports exist regarding the adhesion energy between silica and lipid membranes.

Anderson et al. measured force−distance curves between silica and phospholipid membranes in two different environments.[57] In ultrapure water, they found a repulsion regime between the membrane and silica. In buffered physiological salt concentrations, the silica−membrane interaction is attractive, as repelling charges are shielded by ions. The adhesion energy of silica to DMPC in the fluid phase is reported to be around 0.5−1 mJ/m^2. However, adhesion energies ranging from 10^{-5} to 1 mJ/m^2 are well-known under different conditions,[57,58] where adhesion can be measured without contact in the weak and ultraweak regimes.[59,60]

A study of our group regarding the ion concentration switching on and off the adhesion energy was reported by Wittman et al.[61] For a supported lipid bilayer in the fluid phase (DOPC) and a micrometer-sized silica bead, we found a salt-dependent attraction threshold value, at about $c_{crit} = 15$ mM NaCl. At higher salt concentrations, the adhesion energy saturates at about $E_{adh} = 60$ μJ/m^2, being significantly smaller than the one cited above. The threshold ion concentration of the adhesion energy between silica and lipid membranes obviously should play a role in NP uptake of GUV from model membranes. Indeed, such a threshold value of the salt concentration for the uptake of NP as a function of particle size has been identified by Strobl et al.: for particles with a diameter of $d = 60$ nm and DOPC GUV, NP uptake occurs only above a threshold of about $c_{crit} = 15$ mM.[24] After all, to the best of our knowledge, the adhesion energy has so far not been measured in the gel state at nonzero salt conditions.

Another important thermodynamic interaction aspect has been reported by us earlier. For attractive NP−membrane interaction, we found that silica NP directly shift the melting transition temperature of the wrapping membrane.[26] In the case of a supported lipid bilayer, this effect asymmetrically affects the two bilayer leaflets, causing individual leaflet melting.[62] Strobl et al. applied this to direct NP uptake measurements and expanded this mechanistic model by adding a thermodynamic perspective.[25] Surprisingly, not only NP−membrane interactions are altered, but membrane−membrane adhesion forces are too. These forces include membrane undulation forces, which are tension-dependent. During NP uptake, tension rises as the membrane is consumed, and water incompressibility keeps the vesicle volume constant. However, pores allow fluid to escape the vesicle and relieve tension. The balance of these processes highly depends on pore lifetime, which is strongly dependent on the membrane state and is prolonged near the main phase transition of the membranes.

Strobl et al.[24,25] extended the model of Deserno et al. and simulation results identified an additional regime where nearly unlimited NP uptake appears. They also provided a first experimental glimpse into the NP uptake of gel-state vesicles

https://doi.org/10.1021/acs.jpcb.4c02383
J. Phys. Chem. B 2024, 128, 7172−7179

and observed qualitative differences for different NP sizes. However, there is a lack of systematic studies on experimentally determined NP uptake as a function of the phase state. This study addresses this issue by focusing on the variation of the phase state along the temperature axis.

The structure of the paper is as follows: first, we present a typical vesicle shrinkage kinetic, which we measured for various temperatures and fitted linearly. Second, we identify the phase states of the GUV via calorimetry. Third, we regard the quality of the linear fits to identify linear and nonlinear uptake regimes. This is put under perspective of the main outcome of this study, which is the vesicle shrinkage rate as a function of temperature.

METHODS

Nanoparticles. Monodisperse, nonporous silica NP with silanol groups on the NP surface were purchased from nanoComposix (Prague, Czech Republic). The NP were diluted to a final surface area concentration of $C^A = C(4\pi r^2) = 1\ m^2/L$.

Giant Unilamellar Vesicles. 1,2-Dipentadecanoyl-sn-glycero-3-phosphocholine (15:0 PC) dissolved in chloroform was purchased from Avanti Polar Lipids (Alabaster, Alabama, USA). Membrane fluorescent marker 3,3′-ditetradecyloxacarbocyanine (Texas Red DHPE) was purchased (Thermo Fisher Scientific Inc., USA). Buffer ingredients Na2HPO4, NaH2PO4, sucrose, and D-(+)-glucose monohydrate was purchased from Merck (Darmstadt, Germany). For all aqueous solutions, ultrapure water (pure Aqua, Germany) with a specific resistance $\rho \geq 18\ M\Omega$ cm was used.

GUV were produced by the electroformation technique.[70] Briefly, lipids ($m = 1.26$ mg, $n = 1.8\ \mu$mol) were mixed with $c = 0.05$ mol % of the fluorescent marker Texas Red DHPE and diluted in chloroform to a total concentration of $c_m = 10$ mg/mL at a total volume of 126 μL. The lipid solution was spread onto fluorine tin oxide (FTO)-coated glass slides. A thin lipid film formed after solvent evaporation through vacuum extraction. Using the lipid film on the FTO-coated glass slides, a chamber (volume = 6.2 mL) was built, using Teflon spacers. Two holes in in the spacers enabled filling the chamber with vesicle interior medium. Finally, a rectangular AC voltage was applied in two steps, first for $t_1 = 15$ min ($f = 10$ Hz, $E_{eff} = 0.6$ V/mm), then for $t_2 = 4$ h ($f = 10$ Hz, $E_{eff} = 2.4$ V/mm) at 10 K above phase transition temperature. Using the calorimetric measurement (Figure 2) and melting enthalpy ($\Delta H = 31$ kJ/mol) from literature, we estimated a total lipid amount of $m = 0.14$ mg for a volume of 580 μL or $n = 0.2\ \mu$mol. The GUV were transitioned into vials and stored for weeks in the fridge without loss of quality.

At the stage of GUV preparation, the vesicle interior and exterior medium consisted of sucrose solution. The pH was adjusted to pH = 7. Osmolarity was measured (Osmomat 030, Gonotec GmbH, Germany) and eventually adjusted to $c_n = 150$ mM. Concentrations of NP and GUV were kept constant.

Nanoparticle Uptake Setup. A transparent flat-bottom polystyrene 96-well plate was used to prevent unspecific adhesion of the GUV and the substrate. The well plate was mounted on a fluorescence microscope (Axiovert 200M, Carl Zeiss Microscopy, Jena, Germany).

To dilute the GUV and to change the exterior medium, $V = 2\ \mu$L GUV solution were pipetted into a well filled with $V = 70\ \mu$L consisting of $c = 56$ mM NaCl, 20 mM glucose, 18 mM PBS buffer and deionized water. Salt is needed for net NP uptake, as quantitatively studied by our group earlier.[24] GUV are gently mixed and they sediment due to a higher density of the incapsulated sucrose solution.

The temperature was controlled using a microcontroller and a Peltier element. The temperature was measured and monitored in an equivalent adjacent well by a thermocouple. Preheating of the vesicle suspension without NP was applied for 30 min before each experiment to ensure an equilibrated temperature in the well plate. Hence, shrinking due to other factors than NP could be excluded.

The subsequent addition of NP via gentle pipet aspiration mixing initiated the kinetic uptake process. Once the NP are added to the vesicles, they start interacting. The initial interaction is attractive and leads to endocytosis-like uptake, a full wrapping of the NP with the membrane and complete engulfment into the vesicle. As a consequnce the vesicles' diameter shrinks over time, as can be seen in Figure 1. To

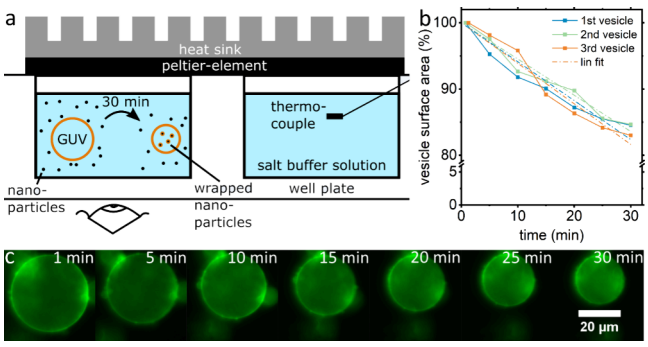

Figure 1. (a) Schematic illustration of the measurement setup. (b) Vesicle area as a function of time ($T = 34$ °C). (c) Fluorescent micrograph time series of a GUV after the addition of nanoparticles ($T = 37$ °C). The vesicle clearly shrinks with ongoing time, due to the uptake of the particles. We used 15:0 PC vesicles with a 1% Texas Red staining and a SiO_2 nanoparticle (diameter $d = 60$ nm) surface concentration of $C^A = 1\ m^2/L$. Preheating and equilibration of the vesicle solution without nanoparticles ensured no shrinkage of the vesicles due to other factors than nanoparticle uptake.

quantify for the uptake, we measured the vesicle surface area through fluorescent imaging with time steps $t_{step} = 5$ min over an overall time period of $t_{total} = 30$ min in case of saturation and $t_{total} = 2$ h in case of no saturation. For each single independent experiment, the shrinkage of a single GUV is recorded.

Figure 1a shows the experimental setup to measure shrinkage kinetics of GUV after the addition of NP. One well of a 96-well plate served as the experimental chamber, whereas an identical adjacent well was used to measure and adjust the temperature using a thermocouple. Once the temperature was equilibrated, we added the NP solution, mixed it gently, and started recording fluorescence micrographs. The time series in Figure 1c exemplarily shows the shrinkage of GUV with ongoing time. We calculated the normalized surface area shrinkage by assuming a spherical shape of the vesicle, as shown in Figure 1b. From the first two data points, we quantify the initial shrinkage rate. Because of the 30 min pre-heating of the vesicle solution without NP in the well plate, shrinking due to other factors than the uptake of NP was excluded.

Data Evaluation. Using an elliptical fit and the isotropic assumption, we determined the surface area for each vesicle at

https://doi.org/10.1021/acs.jpcb.4c02383
J. Phys. Chem. B 2024, 128, 7172−7179

every time step. Preliminary work has shown a transition from linear to exponential decay in shrinkage as a function of time for the present NP size and surface area concentration.[24] We fitted the data linearly but added the adjusted R^2 data to show deviation from linearity. The main parameters are absolute shrinkage, which is a function of temperature.

Differential Scanning Calorimetry. All liquids were degassed prior to the calorimetry (MicroCal VP-DSC, MicroCal Inc., now Malvern Panalytical Ltd., UK) and adjusted to p = 15 psi pressure. A scan rate β = 15 K/h was chosen to ensure a quasi-static process. From three subsequent up and down cycles, only the last up scan was evaluated. The baseline was determined and subtracted as described previously.[71] Concentrated GUV stock solution was used as the DSC sample, for the reference, pure sucrose solution was used.

RESULTS AND DISCUSSION

To compare NP uptake rates and membrane state, it is crucial to measure the excess heat capacity of the used vesicle samples via calorimetry to identify the main phase transition region. Figure 2 shows the measured excess heat capacity $\Delta C_p(T)$ of

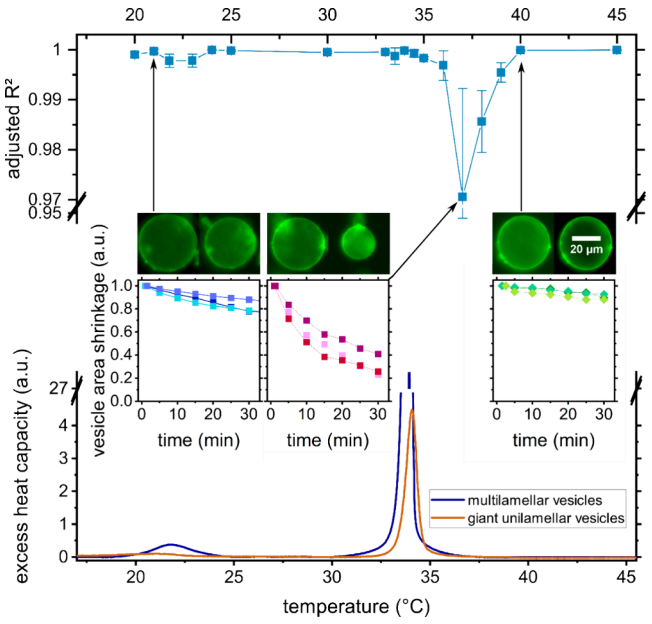

Figure 2. Linear fit quality R^2 (blue squares) as a function of temperature and therefore phase state. The phase state is characterized by the excess heat capacity (orange line). Here, two phase transitions can be identified, a pretransition at T_p = 21.0 °C and the main transition at T_m = 34.1 °C for GUV and 21.8 and 33.9 °C for MLV. The insets show respectively three time series of the NP uptake process represented by the reduction in vesicle surface area, visualized above as fluorescent micrographs.

GUV (orange line) and multilamellar vesicles (MLV) (blue line) of the used lipids. The excess heat capacity of GUV shows a pretransition at T_p = 21.0 °C and the main transition at T_m = 34.1 °C. The broadness of the peaks are $fwhm_p$ = 4.1 K and $fwhm_m$ = 0.7 K, respectively. This is very different from the well-known transition behavior of MLV, which show a more cooperative phase transition. In fact, when comparing the phase transition behavior of GUV to the much smaller large unilamellar vesicles (LUVs) and to rather nonhomogeneous MLV, it was shown that the curvature exerts a minor influence on the broadness of the phase transition compared to the coupling of the bilayers of a MLV.[63] The MLV show a pre and main transition at T_p = 21.8 °C and T_m = 33.9 °C with a width of $fwhm_p$ = 2.3 K and $fwhm_m$ = 0.3 K, respectively, in accordance with literature.[26] Similar values of T_m for MLV and GUV have been reported in the literature for the same lipid with one unit longer acyl-chain length.[63]

Figure 2 furthermore shows the adjusted R^2 value of the linear fits to the shrinkage kinetics as a function of temperature. By far, most data points are close to 1, implying a good accuracy for the linear fit. The linear trend suggests further shrinkage for longer observation time.

Few adjusted R^2 values deviate from 1 in Figure 2, implying a worse accuracy of a linear fit. The inset time series in Figure 2 shows a nonzero curvature indicating an asymptotic, saturating trend. Here, better fitting quality was obtained by fitting exponential functions. However, due to the already relatively high absolute adjusted R^2 value and due to an additional fitting parameter in the exponential function, a comparison is obsolete. Note that the NP uptake kinetics with saturating trends are in proximity of the phase transition regions on the temperature axis, indicating a correlation of phase transition and NP uptake.

The shrinkage of GUV upon NP uptake is driven by a complex interplay of adhesion energy, membrane tension, and pore formation. Adhesion energy, which is influenced by the material properties of the NP and the ionic strength of the surrounding medium, serves as the driving force for the initial binding and subsequent engulfment of NP by the membrane. Membrane tension increases as the vesicle membrane wraps around and internalizes the NP, leading to a reduction in vesicle surface area. This tension rise is moderated by the formation of transient pores, which allow water to escape and relieve some of the built-up tension.[24,25]

To gain a deeper understanding of the kinetic process, we present the time evolution of the vesicle area shrinkage rate as a function of time for four exemplary temperatures close to the pre and main transition in Figure 3a. The results reveal that no vesicle area shrinkage rate time evolution is perfectly constant, as expected from the slope of a linear fit function $y = A_0 - rA_1$, whereas r is the shrinkage rate plotted in Figure 3. Moreover, the shrinkage rate time evolution at T = 37 °C is the only one, which reaches a saturation at around 0.2×10^{-3} per second, as it is constant over 10 min and having therefore reached a steady state. This contradicts the previously presumed saturating trend suggested by the inset in Figure 2 and supports an unlimited NP uptake for at least moderately increased observation times. However, for all other exemplary temperatures, the vesicle area shrinkage rates decline steadily, possibly collapsing entirely for slightly longer observation time. The shrinkage rate as a function of vesicle area as shown in Figure 3b supports this conclusion, as all shrinkage rates approach 0, except at T = 37 °C, which saturates at a value significantly greater than 0, which means, that the vesicles at T = 37 °C potentially can take up even more NP despite already losing a significant amount of membrane area at a near constant rate. To gain a complete picture over the whole temperature spectrum, we completed the data set and presented a summary of the data in Figure 4.

Figure 4 shows the vesicle area shrinkage rates as a function of temperature over the first 10 min of the uptake kinetic (blue squares, linear fit of the kinetic). The values for these vesicle area shrinkage rates as a function of temperature show a

https://doi.org/10.1021/acs.jpcb.4c02383
J. Phys. Chem. B 2024, 128, 7172−7179

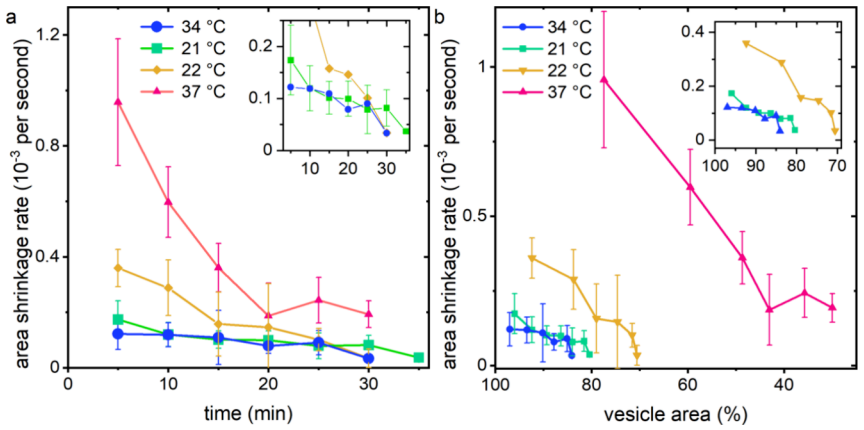

Figure 3. Surface area shrinkage rate of the 15:0 PC GUV due to nanoparticle uptake (a) kinetic and (b) as a function of total vesicle area shrinkage for characteristic temperatures.

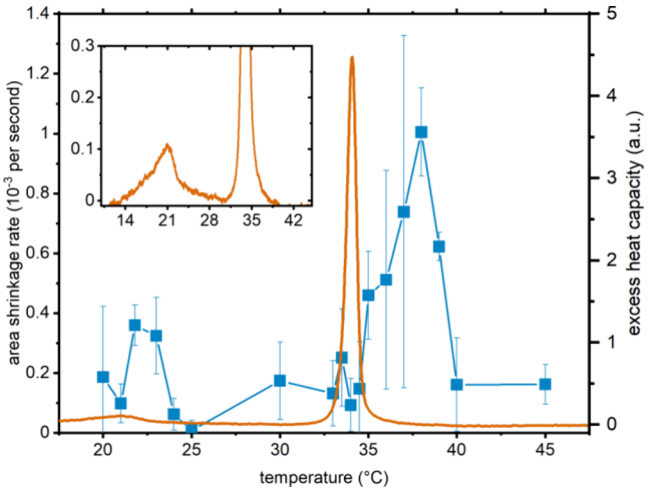

Figure 4. Vesicle area shrinkage rate (blue squares) as a function of temperature and therefore phase state. The phase state characterization of the 15:0 PC GUV by the excess heat capacity has been underlaid for orientation (orange line). The inset shows a zoom of the pre transition.

qualitatively similar shape to the excess heat capacity. The vesicle area shrinkage rates are elevated in proximity to both phase transitions. In both cases, the temperatures, where maximal shrinkage rates appear, are slightly shifted to higher temperature. The local maximal rate close to the pretransition is observed slightly above T_p and the local maximal rate for the main transition is observed at $T_m' = T_m + 3$ K. Besides the obvious correlation of uptake maxima and transition temperatures, it is interesting, that no direct correlation of the magnitudes of heat capacity and shrinkage rate is observed. Consequently, the vesicle area shrinkage rate here close to T_p is more sensitive to structural lipid phase transitions than the excess heat capacity. The existence of even broader transitions in biological membranes[46] and the distribution of membrane order within a population at a constant temperature[64] suggest that the observed influence of the membrane state might play an important role for uptake of NP in cells.

This shift of a response function maximum—which we observe in vesicle area shrinkage rate—in respect to the membrane phase transition temperature of about $\Delta T = +3$ K with respect to T_m has been observed before in the bending energy, down to the exact same $T_{max,bending} = T_m + 3$ K.[40,42,43] However, a high bending modulus impedes NP uptake, contradicting the experimental data. Consequently, the bending energy maximum cannot be the origin of the vesicle area shrinkage rate elevation in the observed shrinkage regime. Note that the bending modulus exhibits dips locally at the phase transition temperatures.[43]

This contradiction can only be resolved by considering further differences in the physical situation, which here is the nanoparticle−membrane interaction. Earlier studies have shown that the chemical potential of the lipid molecules in the membrane is altered when in contact with silica. This interaction shifts the phase transition temperature to $T'_m = T_m - 2.5$ K for 60 nm silica−NP, being NP size dependent.[26,65] However, as the NP interaction stabilizes the fluid phase, the NP uptake peaks should be shifted to lower temperatures, ergo this does not resolve the contradiction, yet.

To understand the interplay of bending and tension as energy-consuming mechanisms and adhesion as an energy-delivering mechanism, the phase state dependency of the membrane tension has to be discussed. The time evolution of membrane tension is strongly dependent on the excess area of the vesicle, the uptake amount and kinetics of NP, as well as the relaxation of tension via volume flux through pores.[66] At the start of our experiments, we can assume zero membrane tension. With increasing uptake, this tension increases as shown earlier.[25] Water can only quickly escape through membrane pores. In addition, it is well-known that close to the main transition the area compressibility is maximal and the pore-forming energy is known to collapse at the phase transition region, due to the inverse proportionality to the isothermal compressibility,[36] resulting in decreased membrane tension around T_m. Moreover, with a constant decrease of membrane area due to engulfment of NP, while the vesicle volume is roughly constant, the rise in tension is proportional to the area compressibility. But in turn, the main transition is sensitive to membrane tension.[67,68] Thus, while a dip in membrane tension around the phase transition region is plausible, fully elucidating the role of membrane tension in the state-dependent NP uptake demonstrated here requires a separate extensive study.

Along the same lines a cautious speculation to understand the observed membrane state dependence of the NP uptake here could be as follows. Close to T_m the adhesion energy might be strongly reduced as compared to the gel and fluid phase. To our knowledge, there are only very few reports in

https://doi.org/10.1021/acs.jpcb.4c02383
J. Phys. Chem. B 2024, 128, 7172−7179

literature quantifying the phase-state-dependent adhesion energy between silica and phospholipid membranes,[67] and especially no classical adhesion energy studies. Thus, in the fluid phase above T_m but in the vicinity to the transition a local maximum in NP uptake could be the consequence of comparably low tension and a decreasing bending modulus with further increasing temperature. However, another study on the adhesion energy as a function of the membrane state is necessary to test this hypothesis.[69]

CONCLUSIONS

In summary, we here showed a strong nonlinear relation between NP uptake rates and temperature for synthetic phospholipid membranes close to the main transition. The phase state of the membrane significantly affects the uptake processes, with notable peaks in NP uptake and vesicle shrinkage rates occurring near phase transition temperatures. At temperatures slightly above the pre and main transition, uptake maxima have been observed. This is understood best by interpreting the mechanical membrane properties as state dependent, nonlinear properties. Thus, membrane properties have to be considered as thermodynamic properties that depend on the membrane state. As in turn, the membrane state close to a main transition can be significantly altered due to direct particle membrane interaction or indirect particle membrane interaction via induced membrane tension, highly nonlinear uptake rates can appear. In addition, these structural transitions are highly sensitive toward changes of the environmental conditions like temperature, shear stress, pH, and other ion concentrations. In turn, in pathophysiological scenarios like inflammation or diets with a high content of polyunsaturated fatty acids such pronounced nonlinear changes in membrane properties could result in pronounced changes in NP uptake. Moreover, it would be highly interesting to pursue the question whether these phenomena are conserved for biological cell membranes as well or if the nonlinear variations of the membrane properties appear over a much wider temperature range and thus in the physiological range appear linear again.

AUTHOR INFORMATION

Corresponding Author

Christoph Westerhausen − *Institute of Theoretical Medicine, Physiology and Institute of Physics, University of Augsburg, Augsburg 86159, Germany; Center for NanoScience (CeNS), Ludwig-Maximilians-Universität Munich, Munich 80799, Germany;* orcid.org/0000-0001-7103-7060; Email: christoph.westerhausen@gmail.com

Authors

Manuel M. Sirch − *Institute of Theoretical Medicine, Physiology and Institute of Physics, University of Augsburg, Augsburg 86159, Germany*

Andrej Kamenac − *Institute of Theoretical Medicine, Physiology and Institute of Physics, University of Augsburg, Augsburg 86159, Germany*

Simon V. Neidinger − *Institute of Theoretical Medicine, Physiology and Institute of Physics, University of Augsburg, Augsburg 86159, Germany;* orcid.org/0009-0004-5115-2693

Achim Wixforth − *Institute of Physics, University of Augsburg, Augsburg 86159, Germany; Center for NanoScience (CeNS), Ludwig-Maximilians-Universität Munich, Munich 80799, Germany*

Complete contact information is available at: https://pubs.acs.org/10.1021/acs.jpcb.4c02383

Notes

The authors declare no competing financial interest.

ACKNOWLEDGMENTS

C.W. would like to acknowledge support by the Center for NanoScience (CeNS) and funding by the DFG (INST 94/135-1 FUGG, 508235635). Moreover, C.W. would like to acknowledge funding for the project "Physical and functional interaction mechanisms at cell membranes and vessel walls" by the University of Augsburg. S.V.N. would like to thank the Hanns-Seidel-Stiftung for financial support. A.K. would like to thank the Joachim Herz Stiftung.

REFERENCES

(1) Buchegger, S.; Kamenac, A.; Fuchs, S.; Herrmann, R.; Houdek, P.; Gorzelanny, C.; Obermeier, A.; Heller, S.; Burgkart, R.; Stritzker, B.; Wixforth, A.; Westerhausen, C. Smart antimicrobial efficacy employing pH-sensitive ZnO-doped diamond-like carbon coatings. *Sci. Rep.* **2019**, *9* (1), 17246.

(2) Buchegger, S.; Vogel, C.; Herrmann, R.; Stritzker, B.; Wixforth, A.; Westerhausen, C. Antibacterial metal ion release from diamond-like carbon modified surfaces for novel multifunctional implant materials. *J. Mater. Res.* **2016**, *31* (17), 2571−2577.

(3) Buchegger, S.; Schuster, N.; Stritzker, B.; Wixforth, A.; Westerhausen, C. Multilayer diamond-like amorphous carbon coatings produced by ion irradiation of polymer films. *Surf. Coat. Technol.* **2017**, *327*, 42−47.

(4) Ettlinger, R.; Sönksen, M.; Graf, M.; Moreno, N.; Denysenko, D.; Volkmer, D.; Kerl, K.; Bunzen, H. Metal−organic framework NP for arsenic trioxide drug delivery. *J. Mater. Chem. B* **2018**, *6* (40), 6481−6489.

(5) Ettlinger, R.; Moreno, N.; Volkmer, D.; Kerl, K.; Bunzen, H. Zeolitic Imidazolate Framework-8 as pH-Sensitive Nanocarrier for 'Arsenic Trioxide' Drug Delivery. *Chem. − Eur. J.* **2019**, *25* (57), 13189−13196.

(6) Ferrari, M. Cancer nanotechnology: opportunities and challenges. *Nat. Rev. Cancer* **2005**, *5* (3), 161−171.

(7) Farokhzad, O. C.; Langer, R. Impact of Nanotechnology on Drug Delivery. *ACS Nano* **2009**, *3* (1), 16−20.

(8) Anselmo, A. C.; Mitragotri, S. NP in the clinic: An update. *Bioeng. Transl. Med.* **2016**, *1* (1), 10−29.

(9) Hajipour, M. J.; Sant, S.; Ashkarran, A.; Laurent, D.; Aghaie, M.; Rahman, H. T. J.; Gonzalez, I.; Mahmoudi, M. Antibacterial properties of nanoparticles. *Trends Biotechnol.* **2012**, *30* (10), 499−511.

(10) Riehemann, K.; Schneider, S. W.; Luger, T. A.; Godin, B.; Ferrari, M.; Fuchs, H. Nanomedicine-Challenge and Perspectives. *Angew. Chemie Int. Ed.* **2009**, *48* (5), 872−897.

(11) Petros, R. A.; DeSimone, J. M. Strategies in the design of NP for therapeutic applications. *Nat. Rev. Drug Discovery* **2010**, *9* (8), 615−627.

(12) Lin, W. Introduction: NP in Medicine. *Chem. Rev.* **2015**, *115* (19), 10407−10409.

(13) McClements, D. J.; Xiao, H. Is nano safe in foods? Establishing the factors impacting the gastrointestinal fate and toxicity of organic and inorganic food-grade nanoparticles. *npj Sci. Food* **2017**, *1* (1), 6.

(14) Donaldson, K.; Tran, L.; Jimenez, L. A.; Duffin, R.; Newby, D. E.; Mills, N.; MacNee, W.; Stone, V. Combustion-derived NP: A review of their toxicology following inhalation exposure. *Part. Fibre Toxicol.* **2005**, *2*, 10.

(15) Merget, R.; Bauer, S.; Küpper, J.; Philippou, M.; Bauer, M.; Breitstadt, D.; Bruening, T. Health hazards due to the inhalation of amorphous silica. *Arch. Toxicol.* **2002**, *75* (11−12), 625−634.
(16) Bauer, A. T.; Strozyk, E. A.; Gorzelanny, C.; Westerhausen, C.; Desch, A.; Schneider, M. F.; Schneider, S. W. Cytotoxicity of silica nanoparticles through exocytosis of von Willebrand factor and necrotic cell death in primary human endothelial cells. *Biomaterials* **2011**, *32* (33), 8385−8393.
(17) Yamashita, K.; Yoshioka, M.; Higashisaka, T.; Mimura, M.; Morishita, T.; Nozaki, Y.; Yoshida, J.; Ogura, Y.; Nabeshi, H.; Abe, Y.; Kamada, H.; Monobe, Y.; Imazawa, T.; Aoshima, H.; Shishido, K.; Kawai, Y.; Mayumi, T.; Tsunoda, S.-i.; Itoh, N.; Yoshikawa, T.; Yanagihara, I.; Saito, S.; Tsutsumi, Y. Silica and titanium dioxide nanoparticles cause pregnancy complications in mice. *Nat. Nanotechnol.* **2011**, *6* (5), 321−328.
(18) Chen, Z.; Meng, H.; Xing, G.; Chen, C.; Zhao, Y.; Jia, G.; Wang, T.; Yuan, H.; Ye, C.; Zhao, F.; Chai, Z.; Zhu, C.; Fang, X.; Ma, B.; Wan, L. Acute toxicological effects of copper nanoparticles in vivo. *Toxicol. Lett.* **2006**, *163* (2), 109−120.
(19) Almeida, J. P. M.; Chen, A. L.; Foster, A.; Drezek, R. In vivo biodistribution of nanoparticles. *Nanomedicine* **2011**, *6* (5), 815−835.
(20) Lesniak, A.; Salvati, A.; Santos-Martinez, M. J.; Radomski, M. W.; Dawson, K. A.; Åberg, C. Nanoparticle Adhesion to the Cell Membrane and Its Effect on Nanoparticle Uptake Efficiency. *J. Am. Chem. Soc.* **2013**, *135* (4), 1438−1444.
(21) Monopoli, M. P.; Walczyk, D.; Campbell, A.; Elia, G.; Lynch, I.; Baldelli Bombelli, F.; Dawson, K. A. Physical−Chemical Aspects of Protein Corona: Relevance to in Vitro and in Vivo Biological Impacts of nanoparticles. *J. Am. Chem. Soc.* **2011**, *133* (8), 2525−2534.
(22) Labouta, H. I.; Asgarian, N.; Rinker, K.; Cramb, D. T. Meta-Analysis of Nanoparticle Cytotoxicity via Data-Mining the Literature. *ACS Nano* **2019**, *13* (2), 1583−1594, DOI: 10.1021/acsnano.8b07562.
(23) Agudo-Canalejo, J.; Lipowsky, R. Critical Particle Sizes for the Engulfment of nanoparticles by Membranes and Vesicles with Bilayer Asymmetry. *ACS Nano* **2015**, *9* (4), 3704−3720.
(24) Strobl, F. G.; Czubak, D. M.; Wixforth, A.; Westerhausen, C. Ion controlled passive nanoparticle uptake in lipid vesicles in theory and experiment. *J. Phys. D. Appl. Phys.* **2019**, *52* (29), No. 294001.
(25) Strobl, F. G.; Seitz, F.; Westerhausen, C.; Reller, A.; Torrano, A. A.; Bräuchle, C.; Wixforth, A.; Schneider, M. F. Intake of silica nanoparticles by giant lipid vesicles: influence of particle size and thermodynamic membrane state. *Beilstein J. Nanotechnol.* **2014**, *5*, 2468−2478.
(26) Westerhausen, C.; Strobl, F. G.; Herrmann, R.; Bauer, A. T.; Schneider, S. W.; Reller, A.; Wixforth, A.; Schneider, M. F. Chemical and mechanical impact of silica nanoparticles on the phase transition behavior of phospholipid membranes in theory and experiment. *Biophys. J.* **2012**, *102* (5), 1032−1038.
(27) Vutukuri, H. R.; Hoore, M.; Abaurrea-Velasco, C.; van Buren, L.; Dutto, A.; Auth, T.; Fedosov, D. A.; Gompper, G.; Vermant, J. Active particles induce large shape deformations in giant lipid vesicles. *Nature* **2020**, *586* (7827), 52−56.
(28) Helfrich, W. Elastic Properties of Lipid Bilayers: Theory and Possible Experiments. *Zeitschrift für Naturforsch. C* **1973**, *28* (11−12), 693−703.
(29) Deserno, M. Elastic deformation of a fluid membrane upon colloid binding. *Phys. Rev. E* **2004**, *69* (3), No. 031903.
(30) Lipowsky, R.; Döbereiner, H.-G. Vesicles in contact with nanoparticles and colloids. *Europhys. Lett.* **1998**, *43* (2), 219−225.
(31) Wunderlich, B.; Leirer, C.; Idzko, A.-L.; Keyser, U. F.; Wixforth, A.; Myles, V. M.; Heimburg, T.; Schneider, M. F. Phase-State Dependent Current Fluctuations in Pure Lipid Membranes. *Biophys. J.* **2009**, *96* (11), 4592−4597.
(32) Ewins, E.; Lira, R. B.; Zhang, W.; Yuan, J.; Antonietti, M.; Robinson, T.; Dimova, R. Poly(Ionic Liquid) Nanoparticles Selectively Disrupt Biomembranes. *Adv. Sci.* **2019**, *6* (4), No. 1801602.
(33) Zhelev, D. V.; Needham, D. Tension-stabilized pores in giant vesicles: determination of pore size and pore line tension. *Biochim. Biophys. Acta - Biomembr.* **1993**, *1147* (1), 89−104.
(34) Teissie, J.; Golzio, M.; Rols, M. P. Mechanisms of cell membrane electropermeabilization: A minireview of our present (lack of ?) knowledge. *Biochim. Biophys. Acta - Gen. Subj.* **2005**, *1724* (3), 270−280.
(35) Gehl, J. Electroporation: Theory and methods, perspectives for drug delivery, gene therapy and research. *Acta Physiol. Scand.* **2003**, *177* (4), 437−447.
(36) Blicher, A.; Wodzinska, K.; Fidorra, M.; Winterhalter, M.; Heimburg, T. The temperature dependence of lipid membrane permeability, its quantized nature, and the influence of anesthetics. *Biophys. J.* **2009**, *96* (11), 4581−4591.
(37) Deserno, M.; Gelbart, W. M. Adhesion and Wrapping in Colloid−Vesicle Complexes. *J. Phys. Chem. B* **2002**, *106* (21), 5543−5552.
(38) Marsh, D. *Handbook of Lipid Bilayers*; CRC Press, 2013.
(39) Heimburg, T. Mechanical aspects of membrane thermodynamics. Estimation of the mechanical properties of lipid membranes close to the chain melting transition from calorimetry. *Biochim. Biophys. Acta - Biomembr.* **1998**, *1415* (1), 147−162.
(40) Fernandez-Puente, L.; Bivas, I.; Mitov, M. D.; Méléard, P. Temperature and Chain Length Effects on Bending Elasticity of Phosphatidylcholine Bilayers. *Europhys. Lett.* **1994**, *28* (3), 181−186.
(41) Méléard, P.; Gerbeaud, C.; Pott, T.; Fernandez-Puente, L.; Bivas, I.; Mitov, M. D.; Dufourcq, J.; Bothorel, P. Bending elasticities of model membranes: influences of temperature and sterol content. *Biophys. J.* **1997**, *72* (6), 2616−2629.
(42) Dimova, R.; Pouligny, B.; Dietrich, C. Pretransitional Effects in Dimyristoylphosphatidylcholine Vesicle Membranes: Optical Dynamometry Study. *Biophys. J.* **2000**, *79* (1), 340−356.
(43) Lee, C.-H.; Lin, W.-C.; Wang, J. All-optical measurements of the bending rigidity of lipid-vesicle membranes across structural phase transitions. *Phys. Rev. E* **2001**, *64* (2), No. 020901(R).
(44) Popescu, G.; Ikeda, T.; Goda, K.; Best-Popescu, C. A.; Laposata, M.; Manley, S.; Dasari, R. R.; Badizadegan, K.; Feld, M. S. Optical Measurement of Cell Membrane Tension. *Phys. Rev. Lett.* **2006**, *97* (21), No. 218101.
(45) Mužić, T.; Tounsi, F.; Madsen, S. B.; Pollakowski, D.; Konrad, M.; Heimburg, T. Melting transitions in biomembranes. *Biochim. Biophys. Acta - Biomembr.* **2019**, *1861* (11), No. 183026.
(46) Färber, N.; Westerhausen, C. Broad lipid phase transitions in mammalian cell membranes measured by Laurdan fluorescence spectroscopy. *Biochim. Biophys. Acta, Biomembr.* **2022**, *1864*, No. 183794, DOI: 10.1016/j.bbamem.2021.183794.
(47) Yamamoto, K.; Ando, J. Endothelial cell and model membranes respond to shear stress by rapidly decreasing the order of their lipid phases. *J. Cell Sci.* **2013**, *126* (5), 1227−1234.
(48) Fedosejevs, C. S.; Schneider, M. F. Sharp, localized phase transitions in single neuronal cells. *Appl. Phys. Sci.* **2022**, *119* (8), No. e2117521119.
(49) Safinya, C. R.; Sirota, E. B.; Roux, D.; Smith, G. S. Universality in interacting membranes: The effect of cosurfactants on the interfacial rigidity. *Phys. Rev. Lett.* **1989**, *62* (10), 1134−1137.
(50) Szleifer, I.; Kramer, D.; Ben-Shaul, A.; Gelbart, W. M.; Safran, S. a. Molecular theory of curvature elasticity in surfactant films. *J. Chem. Phys.* **1990**, *92* (11), 6800.
(51) Evans, E.; Kwok, R. Mechanical calorimetry of large dimyristoylphosphatidylcholine vesicles in the phase transition region. *Biochemistry* **1982**, *21* (20), 4874−4879.
(52) Anthony, F. H.; Biltonen, R. L.; Freire, E. Modification of a vibrating-tube density meter for precise temperature scanning. *Anal. Biochem.* **1981**, *116* (1), 161−167.
(53) Shrivastava, S.; Schneider, M. F. Opto-Mechanical Coupling in Interfaces under Static and Propagative Conditions and Its Biological Implications. *PLoS One* **2013**, *8* (7), No. e67524.
(54) Steppich, D.; Griesbauer, J.; Frommelt, T.; Appelt, W.; Wixforth, A.; Schneider, M. Thermomechanic-electrical coupling in

phospholipid monolayers near the critical point. *Phys. Rev. E* **2010**, *81* (6), No. 061123.
(55) Evans, E.; Rawicz, W. Entropy-driven tension and bending elasticity in condensed-fluid membranes. *Phys. Rev. Lett.* **1990**, *64* (17), 2094−2097.
(56) Dietrich, C.; Angelova, M.; Pouligny, B. Ahesion of Latex Spheres to Giant Phospholipid Vesicles: Statics and Dynamics. *J. Phys. II Fr.* **1997**, *7*, 1651−1682.
(57) Anderson, T. H.; Min, Y.; Weirich, K. L.; Zeng, H.; Fygenson, D.; Israelachvili, J. N. Formation of Supported Bilayers on Silica Substrates. *Langmuir* **2009**, *25* (12), 6997−7005.
(58) Schönherr, H.; Johnson, J. M.; Lenz, P.; Frank, C. W.; Boxer, S. G. Vesicle Adsorption and Lipid Bilayer Formation on Glass Studied by Atomic Force Microscopy. *Langmuir* **2004**, *20* (26), 11600−11606.
(59) Gruhn, T.; Franke, T.; Dimova, R.; Lipowsky, R. Novel Method for Measuring the Adhesion Energy of Vesicles. *Langmuir* **2007**, *23* (10), 5423−5429.
(60) Vishnyakov, A.; Li, T.; Neimark, A. V. Adhesion of Phospholipid Bilayers to Hydroxylated Silica: Existence of Nanometer-Thick Water Interlayers. *Langmuir* **2017**, *33* (45), 13148−13156.
(61) Wittmann, C. G.; Kamenac, A.; Strobl, F. G.; Czubak, D.; Wixforth, A.; Westerhausen, C. Ionic strength and the supporting material strongly influence the adhesion of silica to supported lipid bilayers. *Adv. Biosyst.* **2018**, *2*, No. 1800087, DOI: 10.1002/adbi.201800087.
(62) Charrier, A.; Thibaudau, F. Main phase transitions in supported lipid single-bilayer. *Biophys. J.* **2005**, *89* (2), 1094−1101.
(63) Kreutzberger, M. A.; Tejada, E.; Wang, Y.; Almeida, P. F. GUVs Melt Like LUVs: The Large Heat Capacity of MLVs Is Not Due to Large Size or Small Curvature. *Biophys. J.* **2015**, *108* (11), 2619−2622.
(64) Färber, N.; Reitler, J.; Schäfer, J.; Westerhausen, C. Transport Across Cell Membranes is Modulated by Lipid Order. *Adv. Biol.* **2023**, *7* (6), No. e2200282.
(65) Naumann, C.; Brumm, T.; Bayerl, T. M. Phase transition behavior of single phosphatidylcholine bilayers on a solid spherical support studied by DSC, NMR and FT-IR. *Biophys. J.* **1992**, *63* (5), 1314−1319.
(66) Deserno, M.; Gelbart, W. Adhesion and Wrapping in Colloid−Vesicle Complexes. *J. Phys. Chem. B* **2002**, *106*, 5543−5552.
(67) Kong, X.; Qin, S.; Lu, D.; Liu, Z. Surface tension effects on the phase transition of a DPPC bilayer with and without protein: a molecular dynamics simulation. *Phys. Chem. Chem. Phys.* **2014**, *16* (18), 8434−8440.
(68) Chen, D.; Santore, M. M. Large effect of membrane tension on the fluid-solid phase transitions of two-component phosphatidylcholine vesicles. *Proc. Natl. Acad. Sci. U. S. A.* **2014**, *111* (1), 179−184.
(69) Lai, A. C.-k.; Wan, K.-t.; Chan, V. Substrate-induced deformation and adhesion of phospholipid vesicles at the main phase transition. *Biophys. Chem.* **2002**, *99*, 245−258.
(70) Angelova, M. I.; Soléau, S.; Méléard, Ph.; Faucon, F.; Bothorel, P. Preparation of giant vesicles by external AC electric fields. Kinetics and applications. *Prog. Colloid Polym. Sci.* **1992**, *89*, 127−131.
(71) Heimburg, T. *Thermal Biophysics of Membranes*; Wiley-VCH Verlag GmbH & Co. KGaA: Weinheim, 2007; vol 8, no 7.

https://doi.org/10.1021/acs.jpcb.4c02383
J. Phys. Chem. B 2024, 128, 7172−7179